# Deep structural analysis of novel BGaN material layers grown by MOVPE

S. Gautier, G. Patriarche, T. Moudakir, M. Abid, G. Orsal, K. Pantzas, David Troadec, A. Soltani, L. Largeau, O. Mauguin, et al.

# Deep structural analysis of novel BGaN material layers grown by MOVPE

S. Gautier [a,*], G. Patriarche [b], T. Moudakir [c], M. Abid [d], G. Orsal [a], K. Pantzas [d], D Troadec [e], A. Soltani [e], L. Largeau [b], O. Mauguin [b], A. Ougazzaden [d]

[a] LMOPS, EA 4423, Université Paul Verlaine de Metz and Supelec, 2 rue E. Belin, F-57070 Metz, France
[b] LPN CNRS, UPR, Route de Nozay, F-91460 Marcoussis, France
[c] Supelec, UMI 2958GT-CNRS, 2-3 rue Marconi F-57070 Metz, France
[d] Georgia Institute of Technology/GTL, UMI 2958GT-CNRS, 2-3 rue Marconi F-57070 Metz, France
[e] IEMN, UMR CNRS 8520, Université des Sciences et Technologies de Lille, F-59000 Lille, France

BGaN ternary alloys with 0.7% and 1.7% boron grown on GaN/sapphire template substrates by metalorganic vapour phase epitaxy (MOVPE) have been investigated through HAADF-STEM. At low boron content, 0.7%, no compositional fluctuations were observed with XRD or STEM measurements. Photoluminescence at room temperature was measured. At higher boron content, cubic BGaN nano-sized clusters were identified. The clusters are 3 nm wide, homogeneously distributed in size and in density and coherent with the surrounding wurtzite BGaN matrix. Their boron composition was estimated by EDX.

## 1. Introduction

The development of (Al,Ga,In)N nitride materials has given rise to a new generation of opto- and micro-electronic devices. However, there is still room for innovation in this field by exploring boron nitride-based alloys. For instance, boron nitride (BN) has numerous unique properties, i.e. high-temperature-induced electrical conductivity, high mechanical resistance, exceptional chemical stability, short chemical bond length, radiation resistance and optical transparency in a wide spectral range. B(Al,Ga,In)N alloys have been recently proposed in order to take advantage of these properties. Specific applications of such alloys currently under development are: (i) BAlGaN based active regions for UV-optoelectronic devices on AlN or SiC substrates [1], (ii) BAlGaN nuclear detectors, taking advantage of the high sensitivity of the boron atoms to gamma radiation [2] and (iii) BInGaN based third generation solar cells [3] in the visible range, potentially grown lattice-matched on GaN or ZnO template substrates.

In spite of numerous interesting applications, there are several challenges involving the growth of B(Al,Ga,In)N alloys. Since BN is highly dissimilar to GaN, InN and AlN in terms of lattice constant or stable crystalline phase, it is commonly accepted that randomly distributed B(Al,Ga,In)N alloys are not attainable above a few percents of boron. Several papers have investigated the boron incorporation limit, above which a spinodal decomposition occurs in the BGaN material. Typical computed values were reported to be between 0.9% and 5% [4,5]. These values are in agreement with experimental findings, explaining why successful growth of BGaN alloys is achieved only for small boron content: 3.6% by MOVPE and 4.6% by molecular beam epitaxy (MBE) [6,4]. Even though growth conditions can be optimized to limit the impact of miscibility gaps and improve the material quality, a better understanding of the alloy's structural properties will help to further improve boron incorporation as well as to achieve a better understanding of the optical and electrical properties of BGaN.

In this work, the structural properties of low-boron-content BGaN layers at the atomic scale were investigated experimentally.

## 2. Experiment

BGaN layers were grown on 3.5 μm thick *c*-plane-GaN/sapphire templates by MOVPE. Epitaxial growth was performed in a T-shaped reactor [7] using 100% nitrogen as the carrier gas and trimethylgallium (TMG), triethylboron (TEB) and ammonia ($NH_3$) as precursors for gallium, boron and nitrogen, respectively. The growth of the BGaN layers was performed at 1000 °C, with a V/III ratio of 830 and a reactor pressure of 133 hPa (100 Torr). Grown layers were between 400 nm and 1 μm thick. The molar ratio of TEB in the vapour phase, TEB/(TMG+TEB), was varied from 1% to 4%. The boron content of the BGaN samples was determined through HR-XRD $2\theta/\theta$ scans. Asymmetrical $2\theta$ /$\theta$ scans showed that the layers were fully relaxed. As a result, the composition of the samples was deduced from Vegard's law using the following lattice parameters: $c_{BN}=2.55$ °A and $c_{GaN}=5.185$ °A.

* Corresponding author.
*E-mail address:* simon.gautier@metz.supelec.fr (S. Gautier).

The room temperature photoluminescence of the BGaN layers was measured, using a 244 nm SHG argon–ion laser. High resolution transmission electron microscopy (HR-TEM), aberration-corrected scanning TEM (STEM) and atomic-resolution high angle annular dark field (HAADF) STEM images with EDX spectroscopy were combined to determine the structural and chemical nature of the grown films. All the transmission electron microscopy images were taken along the $\langle 1\,1-2\,0\rangle$ zone axis.

## 3. Results and discussion

Two BGaN compositions (B=0.7% and 1.7%) were chosen for the TEM study to illustrate the structural properties of the material.

Fig. 1 shows a HAADF-STEM image of the 0.7% B content layer. For clarity, GaN template substrate layer has been marked on the figure. A columnar structure is observed, each column consisting of a grain of about 100 nm in width. The lateral size of the grains measured on this sample is in good agreement with the one measured by top view atomic force microscopy (AFM) scans. It confirms that the growth happened in a three-dimensional mode. The contrast of the BGaN layer is relatively homogeneous, and comparable to that of GaN, suggesting that there is no compositional inhomogeneity in the layer as HAADF is sensitive to the local atomic number of the atoms. Nevertheless, clearer lines perpendicular to the growth direction segment the columns on the entire width. To investigate the nature of these defects, atomic resolution HAADF images, with Fourier transform analysis, have been realized on the $B_{0.007}Ga_{0.993}N$ layer (Fig. 2a). As observed on the Fourier transform pattern given in Fig. 2b, the different spots correspond to the superposition of both zinc-blende (ZB) and wurtzite (W) patterns. By first selecting the cubic phase reflections and then applying an inverse Fourier transform, the original image was reconstructed, with only the contribution of the ZB phase on the image (highlighted in Fig. 2c). The ZB structured insertions were found to be from two to a few monolayers thick, which corresponds to the elementary ABC atomic stacking characteristic of the cubic phase.

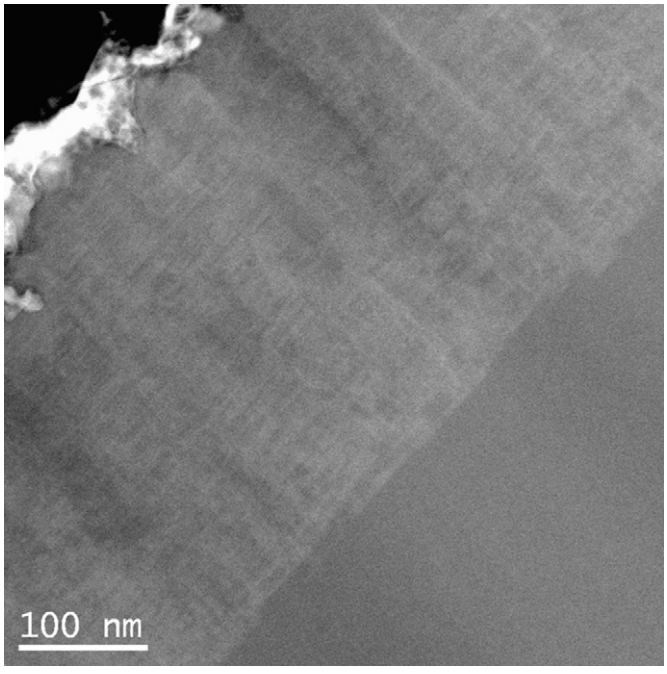


**Fig. 1.** HAADF-STEM picture of a 400 nm thick BGaN layer containing 0.7% of boron (zone axis is 1 1 −2 0).

These observations are in good agreement with the HR-XRD $2\theta/\theta/\omega$ map measurement in the 002 reflection shown in Fig. 3. On the map, two spots are visible. The lower one, more intense, corresponds to the thick GaN layer of the template. The upper spot corresponds to the BGaN layer. The spot is spread much more laterally in omega (FWHM=0.4°) than vertically along $2\theta$ /$\theta$ (FWHM=0.1°). This lateral broadening is due to geometrical defects of the lattice (stacking faults) and not due to compositional inhomogeneity. This observation is reinforced by the homogeneous HAADF contrast all over the epitaxial layer.

Fig. 4 depicts the photoluminescence spectra of the 0.7% boron BGaN sample considered in this study compared to a pure GaN reference. The luminescence of the $B_{0.007}Ga_{0.993}N$ layer peaked at 366 nm, with a red-shift compared to GaN at 362 nm, i.e. a decrease of the bandgap, which is in good agreement with previous work [8]. The lower intensity observed for the $B_{0.007}Ga_{0.993}N$ layer peak can be explained by the presence of numerous stacking faults that we identified in the matrix [9]. Increasing the boron content to 1.7% caused the luminescence intensity to vanish—this is likely due to additional features in the lattice that will be discussed below.

The 1 μm thick BGaN layer containing 1.7% of boron was examined using a similar procedure. The HAADF-STEM image (Fig. 5) shows a columnar growth of the material, the lateral size of the columns being 100 nm. Again, the lateral size of the grains that is observed on TEM cross section was confirmed by the surface measurements performed by AFM. The "chevron" shape of the growth observed on the image is due to small disorientations between the columnar grains observed in this boron rich layer.

In addition to the columnar growth that has already been observed for the lower boron content of 0.7%, the $B_{0.017}Ga_{0.983}N$ sample contains numerous nano-sized clusters (some of them are pointed by arrows in the TEM picture of Fig. 5). Their distribution appears uniform in density laterally and along the growth direction. The clusters range from about 2 to 6 nm in size, with a mean lateral size of $\sim$3 nm. The density of clusters has been estimated to be $\sim 10^4\,\mu m^{-3}$. As a result, the ratio of the volume occupied by the clusters to the total crystal volume represents about 5%.

The structural and chemical nature of individual clusters was investigated by means of HAADF-STEM and EDX. Fig. 6a, a HAADF-STEM image, depicts one isolated nano-sized cluster. A cluster with a larger size (6 nm) than the average was chosen to simplify signal analysis.

Direct Fourier transform was applied to the image in order to reveal the reflections of the crystal structure. Results are shown in Fig. 6b. Both Wurtzite and zinc-blende phase patterns were identified. It is important to note that the zinc-blende insertions and clusters are coherent with the surrounding wurtzite matrix (the 111 reflection of the cubic phase is perfectly aligned with the 0002 refection of the wurtzite hexagonal phase along the growth axis). Fig. 6c and d as reconstructed by singling out the specific wurtzite and zinc-blende reflections and therefore represents, respectively, the contributions of the wurtzite and the zinc-blende phases,which show in each picture as brighter areas. The material contains both crystal phases, the first being complementary to the second on the inverse Fourier transform images. As a result we concluded that the clusters were composed of ZB-BGaN, coherently embedded in the W-BGaN material.

The darker contrast detected by HAADF-STEM on the cubic cluster in Fig. 6a suggests that the local equivalent atomic number ($Z$) changes dramatically to lower values, which is equivalent to higher boron incorporation in the lattice. EDX analysis was used in order to clarify the origin of the HAADF contrast. As no particular impurities (O, C nor Si) were detected that could be responsible for the HAADF dark contrast, it was attributed to the presence of boron. In fact, this light element cannot be detected

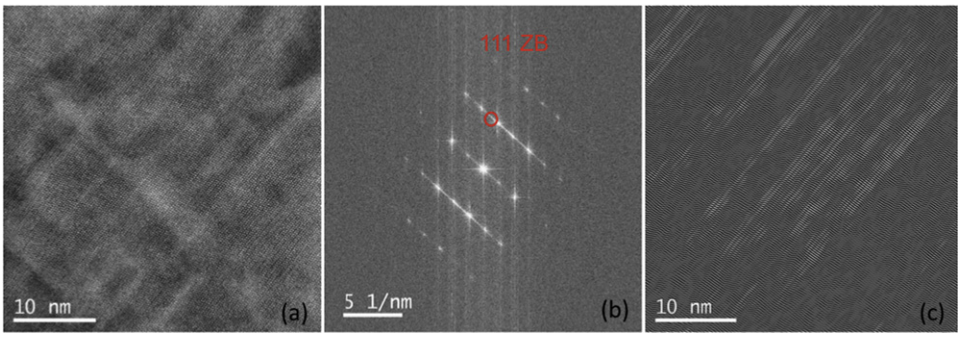


**Fig. 2.** (a): HAADF-STEM picture of a 400 nm thick BGaN layer containing 0.7% of boron. (zone axis is $\langle 1\,1\,-2\,0 \rangle$) and (b) 2D Fourier transform pattern of the HAADF-STEM image of Fig. 2a. The wurtzite reflections as well as the zinc-blende one are present. The specific 111 ZB is circled in red. (c) The BGaN layer image reconstructed by mean of inverse Fourier transform evidences zinc-blende insertions in the BGaN material. (For interpretation of the references to colour in this figure legend, the reader is referred to the web version of this article.)

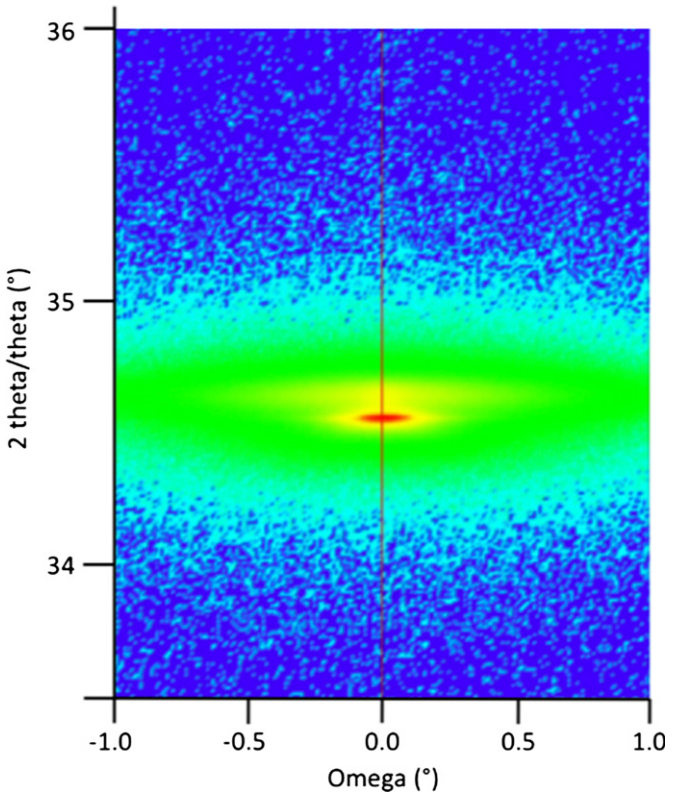


**Fig. 3.** HR-XRD $2\theta/\theta/\omega$ map in the 002 reflection of the 400 nm thick $B_{0.007}Ga_{0.993}N$ layer.

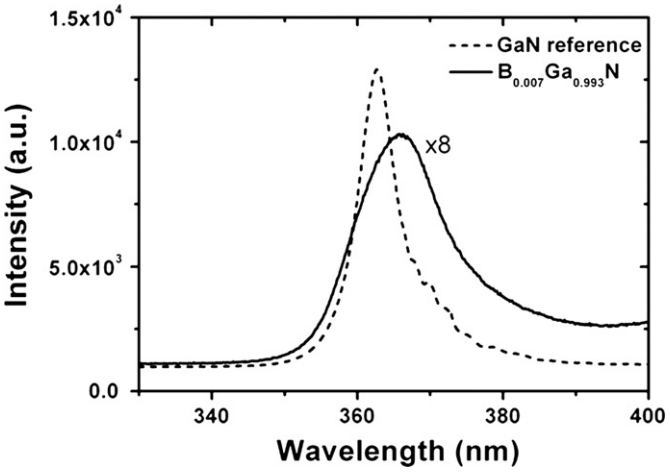


**Fig. 4.** Photoluminescence spectra of BGaN/GaN samples used for this study compared to a GaN reference sample.

by EDX. Despite this problem, the composition was estimated by measuring gallium and considering the stoichiometry between the III and V elements. Within the accuracy of this method, the composition was about $20 \pm 2\%$ of boron inside the cubic clusters.

## 4. Conclusion

In summary, we report low scale HAADF-STEM analysis of BGaN layers grown on GaN template. For high boron content (1.7%), zinc-blende BGaN clusters were found. They were coherent with the matrix and contained approximately 20% of boron and were uniformly distributed in density and size. The clusters represent 5% of the total volume and the 95% remaining BGaN alloy has a uniform boron content.

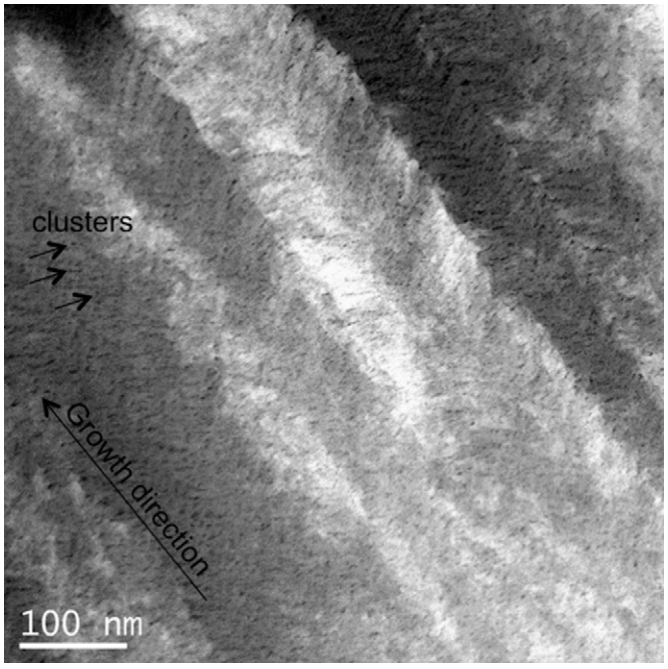


**Fig. 5.** HAADF-STEM picture of a 1 μm thick BGaN layer containing 1.7% of boron.

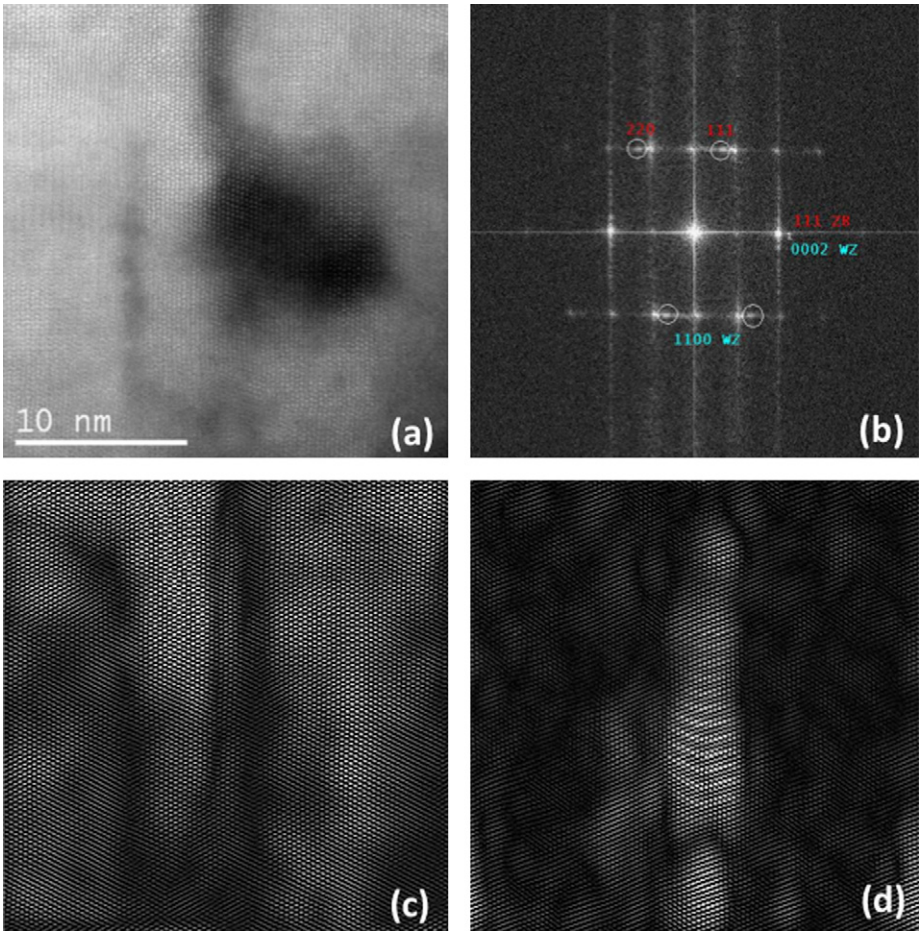


**Fig. 6.** (a) HAADF-STEM picture of a single cluster in a 1000 nm thick BGaN layer containing 1.7% of boron (the thin foil was prepared along the $\langle 1\,1-2\,0\rangle$ zone axis), (b) diffraction pattern of the image. Wurtzite pattern as well as zinc-blende are present, (c) inverse fourrier transform image realized with the specific wurtzite spots 1100 and 11–20 and (d) inverse Fourrier transform picture obtained with the cubic $-1$–11 and 220 spots.

At the lower concentration of boron (0.7%), the growth was columnar but the chemical composition was homogeneous. Numerous stacking faults were identified. Nevertheless, the crystalline quality was good enough to observe room temperature photoluminescence.

## Acknowledgments

The authors would like to acknowledge Vinod Ravindran and Chistopher Bishop for photoluminescence measurements. This work was supported by the French National Research Agency (ANR, GABORE program).

## References

[1] S. Sakai, Y. Ueta, Y. Terauchi, Jpn. J. Appl. Phys. 32 (1993) 4413.
[2] D.S. McGregor, T.C. Unruh, W.J. McNeil, Nucl. Instrum. Methods A 591 (2008) 530–533.
[3] O. Jani, I. Ferguson, C. Honsberg, S. Kurtz, Appl. Phys. Lett. 91 (2007) 132117.
[4] V. Vezin, S. Yatagai, H. Shiraki, S. Uda, Jpn. J. Appl. Phys. 36 (2) (1997) L1483.
[5] L. Escalanti, G.L.W. Hart, Appl. Phys. Lett. 84 (2004) 705.
[6] A. Ougazzaden, S. Gautier, C. Sartel, N. Maloufi, J. Martin, F. Jomard, J. Cryst. Growth 298 (2007) 316.
[7] S. Gautier, C. Sartel, S. Ould-Saad, J. Martin, A. Sirenko, A. Ougazzaden, J. Cryst. Growth 298 (2007) 428.
[8] A. Ougazzaden, S. Gautier, T. Moudakir, Z. Djebbour, Z. Lochner, S. Choi, H.J. Kim, J.-H. Ryou, R.D. Dupuis, A.A. Sirenko, Appl. Phys. Lett. 93 (2008) 083118.
[9] M.A. Reshchikov, H. Morkoc, J. Appl. Phys. 97 (2005) 061301.